

Darboux transformation, positon solution, and breather solution of the third-order flow Gerdjikov-Ivanov equation

Shuzhi Liu(刘树芝), Ning-Yi Li(李宁逸), Xiaona Dong(董晓娜), and Maohua Li(李茂华)

Citation: Chin. Phys. B, 2025, 34 (**1**): 010201. DOI: 10.1088/1674-1056/ad8ec6
Journal homepage: http://cpb.iphy.ac.cn; http://iopscience.iop.org/cpb

What follows is a list of articles you may be interested in

Asymptotic analysis on bright solitons and breather solutions of a generalized higher-order nonlinear Schrödinger equation in an optical fiber or a planar waveguide

Xin Zhao(赵鑫), Zhong Du(杜仲), Li-Jian Zhou(周立俭), Rong-Xiang Liu(刘荣香), and Xu-Hu Wang(王绪虎)
Chin. Phys. B, 2024, 33 (**11**): 110204. DOI: 10.1088/1674-1056/ad7e9e

Dynamics of fundamental and double-pole breathers and solitons for a nonlinear Schrödinger equation with sextic operator under non-zero boundary conditions

Luyao Zhang(张路瑶) and Xiyang Xie(解西阳)
Chin. Phys. B, 2024, 33 (**9**): 090207. DOI: 10.1088/1674-1056/ad6258

Multi-soliton solutions of coupled Lakshmanan-Porsezian-Daniel equations with variable coefficients under nonzero boundary conditions

Hui-Chao Zhao(赵会超), Lei-Nuo Ma(马雷诺), and Xi-Yang Xie(解西阳)
Chin. Phys. B, 2024, 33 (**8**): 080201. DOI: 10.1088/1674-1056/ad4d64

Multi-soliton solutions, breather-like and bound-state solitons for complex modified Korteweg-de Vries equation in optical fibers

Zhong-Zhou Lan(兰中周)
Chin. Phys. B, 2024, 33 (**6**): 060201. DOI: 10.1088/1674-1056/ad39d7

Resonant interactions among two-dimensional nonlinear localized waves and lump molecules for the (2+1)-dimensional elliptic Toda equation

Fuzhong Pang(庞福忠), Hasi Gegen(葛根哈斯), and Xuemei Zhao(赵雪梅)
Chin. Phys. B, 2023, 32 (**5**): 050205. DOI: 10.1088/1674-1056/acb2c2

Darboux transformation, positon solution, and breather solution of the third-order flow Gerdjikov–Ivanov equation

Shuzhi Liu(刘树芝)[1], Ning-Yi Li(李宁逸)[3], Xiaona Dong(董晓娜)[2], and Maohua Li(李茂华)[2,†]

[1] *School of Statistics and Data Science, Ningbo University of Technology, Ningbo* 315211, *China*
[2] *School of Mathematics and Statistics, Ningbo University, Ningbo* 315211, *China*
[3] *College of Wealth and Management, Ningbo University of Finance and Economics, Ningbo* 315175, *China*

(Received 30 August 2024; revised manuscript received 12 October 2024; accepted manuscript online 5 November 2024)

The third-order flow Gerdjikov–Ivanov (TOFGI) equation is studied, and the Darboux transformation (DT) is used to obtain the determinant expression of the solution of this equation. On this basis, the soliton solution, rational solution, positon solution, and breather solution of the TOFGI equation are obtained by taking zero seed solution and non-zero seed solution. The exact solutions and dynamic properties of the Gerdjikov–Ivanov (GI) equation and the TOFGI equation are compared in detail under the same conditions, and it is found that there are some differences in the velocities and trajectories of the solutions of the two equations.

Keywords: third-order flow Gerdjikov–Ivanov equation, solitons, positons, breathers

PACS: 02.30.Jr, 02.30.Ik, 04.20.Jb

DOI: 10.1088/1674-1056/ad8ec6 **CSTR:** 32038.14.CPB.ad8ec6

1. Introduction

The soliton theory is an important branch of nonlinear science. It provides important mathematical models for optical fiber communication, plasma physics, solid state physics, hydrodynamics, and other fields. Therefore, it has attracted the interest of many scholars and a lot of research has been conducted.[1–5] In 1972, Ryogo Hirota revealed the close relationship between classical solitons and envelope solitons by using the Hirota bilinear method with higher-order nonlinear terms.[6] Subsequently, a series of soliton equations with higher-order nonlinear terms have been studied.[7–13] The generalized nonlinear Schrödinger equation with fourth-order dispersion and quintic nonlinear terms was studied in Ref. [14], and it was pointed out that the equation is suitable for short-period pulse propagation in metamaterials with delayed Raman response. With the development of laser and ultra-high bit rate fiber communication technology, high-order nonlinear effects are inevitable in many optical systems. Therefore, it is significant and necessary to explore the influence of higher-order nonlinear effects on nonlinear partial differential equations.

As we know, the derivative nonlinear Schrödinger (DNLS) equation is the modification and generalization of the nonlinear Schrödinger (NLS) equation. There are three types of DNLS equations: the Kaup–Newell equation (KN),[15] the Chen–Lee–Liu equation (CLL)[16] and the Gerdjikov–Ivanov equation (GI).[17] They are also commonly referred to as DNLSI, DNLSI, and DNLSIII, respectively. The GI equation is as follows:

$$\mathrm{i}q_t + q_{xx} - \mathrm{i}q^2 q_x^* + \frac{1}{2}q^3 q^{*2} = 0. \tag{1}$$

The GI equation is a model of the propagation of Alfvén waves parallel to magnetic field environment in plasma physics, where q is the transverse magnetic field disturbance, the symbol '*' represents the complex conjugate, and x and t are the coordinates of space and time, respectively.[18–20] There are some interesting modifications of the GI equation, for example the third-order flow Gerdjikov–Ivanov (TOFGI) equation[21]

$$q_t = -\frac{1}{2}q_{xxx} - \frac{3}{2}\mathrm{i}qq_x q_x^* - \frac{3}{4}|q|^4 q_x. \tag{2}$$

It is found that the higher-order dispersion term of the TOFGI equation can affect the direction, velocity, and amplitude of soliton propagation by using the Riemann–Hilbert method.[21] But the soliton solution, positon solution, and breather solution of the TOFGI equation are also worthy of objects of an integrable system. The Darboux transformation (DT) is a powerful tool to solve integrable equations.[22–27] In this paper, we shall generate various types of solutions of the TOFGI equation by using the DT.

The positon solutions have attracted much attention in recent years. The positon solution is a real nonsingular solution, which was first proposed by Matveev in 1992.[28] In this paper, Matveev pointed out that the positon solution of the modified Korteweg–de Vries (mKdV) equation is obviously related to the transparent potential in quantum physics. Subsequently, the positon solutions have been studied extensively.[29–32] It

†Corresponding author. E-mail: limaohua@nbu.edu.cn

© 2025 Chinese Physical Society and IOP Publishing Ltd. All rights, including for text and data mining, AI training, and similar technologies, are reserved.

is well known that the N-soliton solution can be split apart into the sum of N single soliton solutions and produce a phase shift, which shows that solitons are stable when colliding with each other, and we can identify each soliton in the sense of a particle.[33] The positon solution is degenerated from the soliton solution. So the positon solution is split in this paper and the properties of collision process can be clarified by analyzing phase shift.

The structure of this paper is as follows. The determinant representation of the N-order solution of the TOFGI equation is given in Section 2 (see also Refs. [21,34]), and the formulas of the soliton solution and positon solution are also obtained. In Section 3, the positon solution is split and its dynamic characteristics are analyzed. In Section 4, the breather solution of the TOFGI equation and its three-dimensional profiles are obtained. Finally, the conclusion is given in Section 5.

2. The soliton solution and positon solution of the TOFGI equation

There are extensions of the GI equation, the coupled TOFGI equation,[21]

$$\begin{cases} q_t+\dfrac{1}{2}q_{xxx}+\dfrac{3}{2}\mathrm{i}qq_xr_x+\dfrac{3}{4}q^2r^2q_x=0,\\ r_t+\dfrac{1}{2}r_{xxx}-\dfrac{3}{2}\mathrm{i}rr_xq_x+\dfrac{3}{4}r^2q^2r_x=0. \end{cases} \tag{3}$$

Equation (3) can be reduced to Eq. (2) with constraint $q=-r^*$. This system of coupled equations admits the following Lax pair:[21]

$$\begin{aligned} \phi_x=U\phi &= \left(-\mathrm{i}\lambda^2\sigma_3+\lambda Q-\frac{\mathrm{i}}{2}Q^2\sigma_3\right)\phi,\\ \phi_t=V\phi &= (-2\mathrm{i}\lambda^6\sigma_3+Z_5\lambda^5+Z_4\lambda^4\\ &\quad +Z_3\lambda^3+Z_2\lambda^2+Z_1\lambda+Z_0)\phi, \end{aligned} \tag{4}$$

with

$$\begin{aligned} &\phi(x,t,\lambda)=\begin{pmatrix} f(x,t,\lambda)\\ g(x,t,\lambda)\end{pmatrix},\\ &\sigma_3=\begin{pmatrix}1&0\\0&-1\end{pmatrix},\quad Q=\begin{pmatrix}0&q\\r&0\end{pmatrix},\\ &Z_0=\frac{\mathrm{i}}{4}(QQ_{xx}+Q_{xx}Q)\sigma_3-\frac{\mathrm{i}}{4}Q_x^2\sigma_3+\frac{\mathrm{i}}{8}Q^6\sigma_3,\\ &Z_1=-\frac{1}{2}Q_{xx}+\frac{\mathrm{i}}{2}QQ_xQ\sigma_3-\frac{1}{4}Q^5,\\ &Z_2=-\frac{1}{2}[Q,Q_x]+\frac{1}{4}\mathrm{i}Q^4\sigma_3,\\ &Z_3=\mathrm{i}\sigma_3Q_x,\quad Z_4=-\mathrm{i}Q^2\sigma_3,\quad Z_5=2Q. \end{aligned}$$

Here, $\lambda\in\mathbb{C}$ is the spectral parameter and ϕ is the eigenfunction of Eq, (4) related to λ. The coupled TOFGI equation can be obtained from the zero curvature equation $U_t-V_x+[U,V]=0$.

In order to obtain the solution of the TOFGI equation, it is found that the DT of the GI equation is also applicable to the TOFGI equation through Ref. [34]. The same situation also occurs in the third-order flow equation of the Kaup–Newell system.[35] Thus, the lemma can be obtained as follows.

Lemma 1 Letting $\phi_i=\begin{pmatrix}f_i\\g_i\end{pmatrix}$ be the eigenfunction related to λ_i of the spectral problem, the new solutions of the TOFGI equation are obtained by DT,

$$q^{[n]}=q+2\mathrm{i}\frac{\Omega_{11}}{\Omega_{12}},\quad r^{[n]}=r-2\mathrm{i}\frac{\Omega_{21}}{\Omega_{22}}. \tag{5}$$

(1) For $n=2k$ $(k=1,2,3,\ldots)$,

$$\Omega_{11}=\begin{vmatrix} f_1&\lambda_1g_1&\cdots&\lambda_1^{n-3}g_1&\lambda_1^{n-2}f_1&-\lambda_1^nf_1\\ f_2&\lambda_2g_2&\cdots&\lambda_2^{n-3}g_2&\lambda_2^{n-2}f_2&-\lambda_2^nf_2\\ \vdots&\vdots&\vdots&\vdots&\vdots&\vdots\\ f_n&\lambda_ng_n&\cdots&\lambda_n^{n-3}g_n&\lambda_n^{n-2}f_n&-\lambda_n^nf_n \end{vmatrix},$$

$$\Omega_{12}=\begin{vmatrix} f_1&\lambda_1g_1&\cdots&\lambda_1^{n-3}g_1&\lambda_1^{n-2}f_1&\lambda_1^{n-1}g_1\\ f_2&\lambda_2g_2&\cdots&\lambda_2^{n-3}g_2&\lambda_2^{n-2}f_2&\lambda_2^{n-1}g_2\\ \vdots&\vdots&\vdots&\vdots&\vdots&\vdots\\ f_n&\lambda_ng_n&\cdots&\lambda_n^{n-3}g_n&\lambda_n^{n-2}f_n&\lambda_n^{n-1}g_n \end{vmatrix},$$

$$\Omega_{21}=\begin{vmatrix} g_1&\lambda_1f_1&\cdots&\lambda_1^{n-3}f_1&\lambda_1^{n-2}g_1&-\lambda_1^ng_1\\ g_2&\lambda_2f_2&\cdots&\lambda_2^{n-3}f_2&\lambda_2^{n-2}g_2&-\lambda_2^ng_2\\ \vdots&\vdots&\vdots&\vdots&\vdots&\vdots\\ g_n&\lambda_nf_n&\cdots&\lambda_n^{n-3}f_n&\lambda_n^{n-2}g_n&-\lambda_n^ng_n \end{vmatrix},$$

$$\Omega_{22}=\begin{vmatrix} g_1&\lambda_1f_1&\cdots&\lambda_1^{n-3}f_1&\lambda_1^{n-2}g_1&\lambda_1^{n-1}f_1\\ g_2&\lambda_2f_2&\cdots&\lambda_2^{n-3}f_2&\lambda_2^{n-2}g_2&\lambda_2^{n-1}f_2\\ \vdots&\vdots&\vdots&\vdots&\vdots&\vdots\\ g_n&\lambda_nf_n&\cdots&\lambda_n^{n-3}f_n&\lambda_n^{n-2}g_n&\lambda_n^{n-1}f_n \end{vmatrix}.$$

(2) For $n=2k+1$ $(k=1,2,3,\ldots)$,

$$\Omega_{11}=\begin{vmatrix} g_1&\lambda_1f_1&\cdots&\lambda_1^{n-3}f_1&\lambda_1^{n-2}g_1&-\lambda_1^nf_1\\ g_2&\lambda_2f_2&\cdots&\lambda_2^{n-3}f_2&\lambda_2^{n-2}g_2&-\lambda_2^nf_2\\ \vdots&\vdots&\vdots&\vdots&\vdots&\vdots\\ g_n&\lambda_nf_n&\cdots&\lambda_n^{n-3}f_n&\lambda_n^{n-2}g_n&-\lambda_n^nf_n \end{vmatrix},$$

$$\Omega_{12}=\begin{vmatrix} g_1&\lambda_1f_1&\cdots&\lambda_1^{n-3}f_1&\lambda_1^{n-2}g_1&\lambda_1^{n-1}g_1\\ g_2&\lambda_2f_2&\cdots&\lambda_2^{n-3}f_2&\lambda_2^{n-2}g_2&\lambda_2^{n-1}g_2\\ \vdots&\vdots&\vdots&\vdots&\vdots&\vdots\\ g_n&\lambda_nf_n&\cdots&\lambda_n^{n-3}f_n&\lambda_n^{n-2}g_n&\lambda_n^{n-1}g_n \end{vmatrix},$$

$$\Omega_{21}=\begin{vmatrix} f_1&\lambda_1g_1&\cdots&\lambda_1^{n-3}g_1&\lambda_1^{n-2}f_1&-\lambda_1^ng_1\\ f_2&\lambda_2g_2&\cdots&\lambda_2^{n-3}g_2&\lambda_2^{n-2}f_2&-\lambda_2^ng_2\\ \vdots&\vdots&\vdots&\vdots&\vdots&\vdots\\ f_n&\lambda_ng_n&\cdots&\lambda_n^{n-3}g_n&\lambda_n^{n-2}f_n&-\lambda_n^ng_n \end{vmatrix},$$

$$\Omega_{22}=\begin{vmatrix} f_1&\lambda_1g_1&\cdots&\lambda_1^{n-3}g_1&\lambda_1^{n-2}f_1&\lambda_1^{n-1}f_1\\ f_2&\lambda_2g_2&\cdots&\lambda_2^{n-3}g_2&\lambda_2^{n-2}f_2&\lambda_2^{n-1}f_2\\ \vdots&\vdots&\vdots&\vdots&\vdots&\vdots\\ f_n&\lambda_ng_n&\cdots&\lambda_n^{n-3}g_n&\lambda_n^{n-2}f_n&\lambda_n^{n-1}f_n \end{vmatrix}.$$

Taking the zero seed solution $q=r=0$, the eigenfunc-

tions related to λ_j are as follows:

$$\phi_j = \phi(\lambda_j) = \begin{pmatrix} f(x,t,\lambda_j) \\ g(x,t,\lambda_j) \end{pmatrix} = \begin{pmatrix} \mathrm{e}^{-\mathrm{i}\lambda_j^2 x - 2\mathrm{i}\lambda_j^6 t} \\ \mathrm{e}^{\mathrm{i}\lambda_j^2 x + 2\mathrm{i}\lambda_j^6 t} \end{pmatrix}. \tag{6}$$

The following types of solutions can be obtained.

For $n=1$, letting $\lambda_1^* = -\lambda_1$, $\lambda_1 = \mathrm{i}\beta_1$ $(\beta_1 \in \mathbb{R})$ and $\phi_1 = \begin{pmatrix} f_1 \\ g_1 \end{pmatrix} = \begin{pmatrix} g_1^* \\ f_1^* \end{pmatrix}$, then

$$q^{[1]} = 2\beta_1 \mathrm{e}^{2\mathrm{i}\beta_1^2(x+2\beta_1^4 t)}, \tag{7}$$

which represents a plane wave of constant amplitude.

For $n=2$, letting $\lambda_1 = \alpha_1 + \mathrm{i}\beta_1$ $(\alpha_1, \beta_1 \in \mathbb{R})$, $\lambda_2 = -\lambda_1^*$, and $\phi_1 = \begin{pmatrix} f_1 \\ g_1 \end{pmatrix}$, $\phi_2 = \begin{pmatrix} g_1^* \\ f_1^* \end{pmatrix}$, then one-soliton solution of the TOFGI equation with eigenvalues λ_1 can be obtained

$$q^{[2]} = \frac{8\alpha_1\beta_1 \mathrm{e}^{(2\mathrm{i}\beta_1^2 + 4\alpha_1\beta_1 - 2\mathrm{i}\alpha_1^2)H - 8\mathrm{i}(\beta_1^4 - \alpha_1^4)(\alpha_1^2+\beta_1^2)t}}{(\alpha_1 - \mathrm{i}\beta_1)\mathrm{e}^{8\alpha_1\beta_1 H} + \alpha_1 + \mathrm{i}\beta_1}, \tag{8}$$

with

$$H = 2(3\alpha_1^2 - \beta_1^2)(\alpha_1^2 - 3\beta_1^2)t + x.$$

The peak trajectory of the one-soliton solution on the (x,t) plane is

$$x = -2(3\alpha_1^2 - \beta_1^2)(\alpha_1^2 - 3\beta_1^2)t.$$

Letting $\alpha_1 \to 0$ in Eq. (8), we get a rational solution

$$q_{1-\mathrm{rational}} = -\frac{4\beta_1 \mathrm{e}^{2\mathrm{i}\beta_1^2(2\beta_1^4 t + x)}}{24\mathrm{i}\beta_1^6 t + 4\mathrm{i}\beta_1^2 x - 1}, \tag{9}$$

with an arbitrary real constant β_1. In the (x,t) plane, the peak trajectory of rational solution can be expressed as $x = -6\beta_1^4 t$. The three-dimensional plot and density plot of the two solutions are given in Fig. 1.

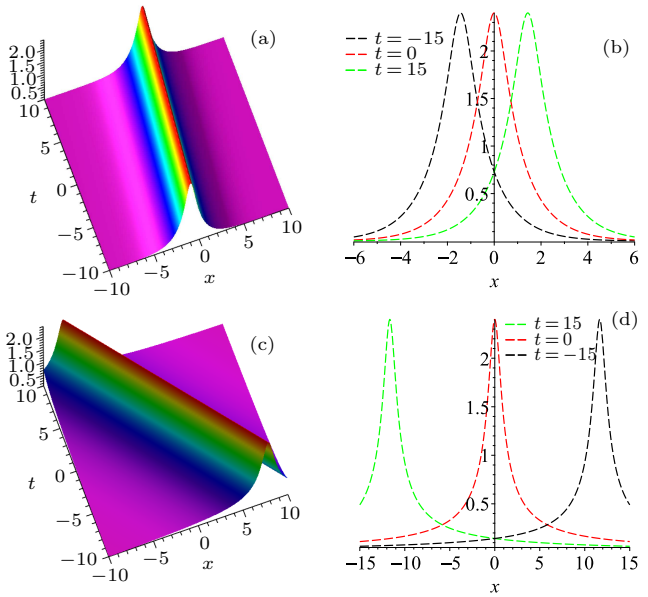


Fig. 1. The dynamic plot of $|q^{[2]}|^2$. (a) and (b) Three-dimensional plot and two-dimensional plot of soliton solutions of the TOFGI equation respectively, with $\alpha_1 = 0.37$, $\beta_1 = 0.6$. (c) and (d) The rational solution three-dimensional and two-dimensional plot of the TOFGI equation, with $\beta_1 = 0.6$.

Remark 1 It can be found from the paper that the peak amplitudes of the one-soliton solution and rational solution of the TOFGI equation and GI equation are equal, which are determined by the value $4\beta_1$. It can be seen from the peak trajectories that the one-soliton solution and the rational solution have different propagation velocities and directions.

For $n=4$, letting $\lambda_1 = \alpha_1 + \mathrm{i}\beta_1$, $\lambda_2 = -\lambda_1^*$, $\lambda_3 = \alpha_3 + \mathrm{i}\beta_3$, $\lambda_4 = -\lambda_3^*$ $(\alpha_1, \alpha_3, \beta_1, \beta_3 \in \mathbb{R})$ and eigenfunction are substituted into Eq. (5), the two-soliton solution of the TOFGI equation can be obtained, and its three-dimensional evolution diagram is shown in Fig. 2(a).

For $n=6$, letting $\lambda_1 = \alpha_1 + \mathrm{i}\beta_1$, $\lambda_2 = -\lambda_1^*$, $\lambda_3 = \alpha_3 + \mathrm{i}\beta_3$, $\lambda_4 = -\lambda_3^*$, $\lambda_5 = \alpha_5 + \mathrm{i}\beta_5$, $\lambda_6 = -\lambda_5^*$ $(\alpha_1, \alpha_3, \alpha_5, \beta_1, \beta_3, \beta_5 \in \mathbb{R})$, taking the same method, the three-soliton solution of the TOFGI equation can be obtained, and its three-dimensional evolution diagram is shown in Fig. 2(b).

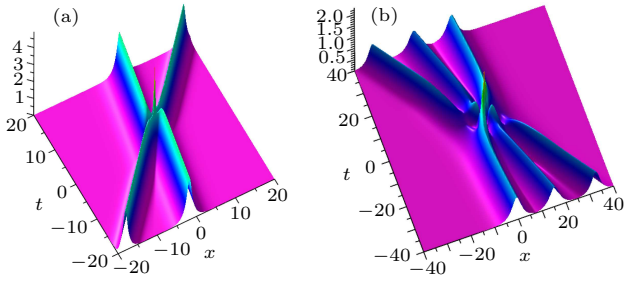


Fig. 2. (a) The three-dimensional plot of the two-soliton solution $|q^{[4]}|^2$ with $\alpha_1 = 0.4$, $\beta_1 = 0.63$, $\alpha_3 = 0.55$, $\beta_3 = 0.6$. (b) The three-dimensional plot of the three-soliton solution $|q^{[6]}|^2$ with $\alpha_1 = 0.52$, $\beta_1 = 0.24$, $\alpha_3 = 0.7$, $\beta_3 = 0.2$, $\alpha_5 = 0.58$, $\beta_5 = 0.22$.

It can be seen from Eq. (5) that when $\lambda_i = \lambda_j$ $(i \neq j)$, the denominator of the N-soliton solution becomes zero. To remedy this defect, the positon solution of the TOFGI equation is solved. The positon solution is a smooth solution obtained by using degenerate DT to approximate the eigenvalues and then using higher order Taylor expansion. Therefore, the following proposition can be obtained.

Proposition 1 Substituting the eigenfunction (6) into Eq. (5) and taking $\lambda_1 = \alpha_1 + \mathrm{i}\beta_1$ $(\alpha_1, \beta_1 \in \mathbb{R})$, $\lambda_2 = -\lambda_1^*$, $\lambda_{2j-1} \to \lambda_1$ and $\lambda_{2j} = -\lambda_{2j-1}^*$ $(j = 2,3,4,\ldots)$, then the degenerate DT is performed. The expression of the N-positon solution can be written as

$$q_{n-p} = 2\mathrm{i}\frac{|\Omega_{11}'|}{|\Omega_{12}'|}, \tag{10}$$

where

$$\Omega_{11}' = \left(\frac{\partial^{n_i - 1}}{\partial \varepsilon^{n_i - 1}} |_{\varepsilon=0} (\Omega_{11})_{ij}(\lambda_1 + \varepsilon) \right)_{2n \times 2n},$$

$$\Omega_{12}' = \left(\frac{\partial^{n_i - 1}}{\partial \varepsilon^{n_i - 1}} |_{\varepsilon=0} (\Omega_{12})_{ij}(\lambda_1 + \varepsilon) \right)_{2n \times 2n},$$

and $n_i = [\frac{i+1}{2}]$, $[i]$ defined as the floor function of i.

Letting $n=2$ in Eq. (10), the two-positon solution can be obtained, whose explicit formula is shown as follows:

$$q_{2-p}=\frac{[\omega_1\sinh(4\alpha_1\beta_1 H)+\omega_2\cosh(4\alpha_1\beta_1 H)]\,\mathrm{e}^{h_1}}{[\omega_3\sinh(4\alpha_1\beta_1 H)+\omega_4\cosh(4\alpha_1\beta_1 H)]\,\mathrm{e}^{12\alpha_1\beta_1 H}+\omega_5}, \tag{11}$$

where

$$\begin{aligned}
H &= 2(3\alpha_1^2-\beta_1^2)(\alpha_1^2-3\beta_1^2)t+x,\\
\omega_1 &= (128-128\mathrm{i})\alpha_1^3\beta_1^2(\alpha_1^2+\beta_1^2)\\
&\quad\times\left[x+6(\alpha_1^4-10\alpha_1^2\beta_1^2+5\beta_1^4)t\right]\\
&\quad+32\alpha_1\beta_1^4(1+\mathrm{i}),\\
\omega_2 &= (-2-2\mathrm{i})\alpha_1^2\beta_1^3(\alpha_1^2+\beta_1^2)\\
&\quad\times\left[64x+193(5\alpha_1^4-10\alpha_1^2\beta_1^2+\beta_1^4)t\right]\\
&\quad+32\alpha_1^4\beta_1(-1+\mathrm{i}),\\
\omega_3 &= \omega_{31}t^2+\omega_{32}xt+\omega_{33}t+\omega_{34}x^2+\omega_{35}x+\omega_{36},\\
\omega_{31} &= (2304-2304\mathrm{i})\alpha_1^2\beta_1^2(\alpha_1^2+\beta_1^2)^6,\\
\omega_{32} &= (768-768\mathrm{i})\alpha_1^2\beta_1^2(\alpha_1^2+\beta_1^2)^2\\
&\quad\times(-\alpha_1^2-2\alpha_1\beta_1+\beta_1^2)(-\alpha_1^2+2\alpha_1\beta_1+\beta_1^2),\\
\omega_{33} &= (192+192\mathrm{i})\alpha_1^2\beta_1^2(\beta_1^2-\alpha_1^2)\\
&\quad\times(\alpha_1^2+4\alpha_1\beta_1+\beta_1^2)(\alpha_1^2-4\alpha_1\beta_1+\beta_1^2),\\
\omega_{34} &= (64-64\mathrm{i})\alpha_1^2\beta_1^2(\alpha_1^2+\beta_1^2)^2,\\
\omega_{35} &= (32+32\mathrm{i})\alpha_1^2\beta_1^2(\beta_1^2-\alpha_1^2),\\
\omega_{36} &= (1-\mathrm{i})\alpha_1^4+(2+2\mathrm{i})\alpha_1^3\beta_1\\
&\quad+(2+2\mathrm{i})\alpha_1\beta_1^3+(3-3\mathrm{i})\beta_1^4,\\
\omega_4 &= \omega_{41}t^2+\omega_{42}xt+\omega_{43}t+\omega_{44}x^2+\omega_{45}x+\omega_{46},\\
\omega_{41} &= -\omega_{31},\quad \omega_{42}=-\omega_{32},\quad \omega_{43}=-\omega_{33},\\
\omega_{44} &= -\omega_{34},\quad \omega_{45}=-\omega_{35},\\
\omega_{46} &= (-3+3\mathrm{i})\alpha_1^4+(2+2\mathrm{i})\alpha_1^3\beta_1\\
&\quad+(2+2\mathrm{i})\alpha_1\beta_1^3+(-1+\mathrm{i})\beta_1^4,\\
\omega_5 &= -[(1-\mathrm{i})\alpha_1^2+(2+2\mathrm{i})\alpha_1\beta_1\\
&\quad+(-1+\mathrm{i})\beta_1^2](\alpha_1^2+\beta_1^2),\\
h_1 &= -4\mathrm{i}(\alpha_1^6-15\alpha_1^4\beta_1^2+15\alpha_1^2\beta_1^4-\beta_1^6)t\\
&\quad-2\mathrm{i}(\alpha_1^2-\beta_1^2)x+8\alpha_1\beta_1 H.
\end{aligned}$$

Letting $\alpha_1\to 0$ in Eq. (11) of the two-positon solution, the second-order rational traveling wave solution of the TOFGI equation can be obtained as follows:

$$q_{2-\mathrm{rational}}=\frac{\beta_1\,\mathrm{e}^{2\mathrm{i}\beta_1^2(2\beta_1^4t+x)}(\tau_{13}t^3+\tau_{12}t^2+\tau_{11}t+\tau_{10})}{\tau_{24}t^4+\tau_{23}t^3+\tau_{22}t^2+\tau_{21}t+\tau_{20}}, \tag{12}$$

where

$$\begin{aligned}
\tau_{13} &= 2^{12}3^3(1+\mathrm{i})\beta_1^{18},\\
\tau_{12} &= 2^9 3^3\beta_1^{12}\left(4(1+\mathrm{i})\beta_1^2x-5(1-\mathrm{i})\right),\\
\tau_{11} &= 2^6 3\beta_1^6(2^4 3(1+\mathrm{i})\beta_1^4x^2-2^3 3^2(1-\mathrm{i})\beta_1^2x-17(1+\mathrm{i})),\\
\tau_{10} &= 2^9(1+\mathrm{i})\beta_1^6x^3-2^7 3(1-\mathrm{i})\beta_1^4x^2\\
&\quad+2^5 3(1+\mathrm{i})\beta_1^2x+2^3 3(1-\mathrm{i}),\\
\tau_{24} &= -2^{12}3^4(1-\mathrm{i})\beta_1^{24},\\
\tau_{23} &= -2^{11}3^3\beta_1^{18}\left(4(1-\mathrm{i})\beta_1^2x+(1+\mathrm{i})\right),\\
\tau_{22} &= -2^7 3^2\beta_1^{12}(2^4 3(1-\mathrm{i})\beta_1^4x^2\\
&\quad+2^3 3(1+\mathrm{i})\beta_1^2x-19(1-\mathrm{i})),\\
\tau_{21} &= -2^5 3\beta_1^6(2^6(1-\mathrm{i})\beta_1^6x^3+2^4 3(1+\mathrm{i})\beta_1^4x^2\\
&\quad+4(1-\mathrm{i})\beta_1^2x+19(1+\mathrm{i})),\\
\tau_{20} &= -2^8(1-\mathrm{i})\beta_1^8x^4-2^8(1+\mathrm{i})\beta_1^6x^3\\
&\quad+2^5 3(1-\mathrm{i})\beta_1^4x^2-2^4 3(1+\mathrm{i})\beta_1^2x+3(1-\mathrm{i}).
\end{aligned}$$

The second-order rational traveling solution is generated, see Fig. 3.

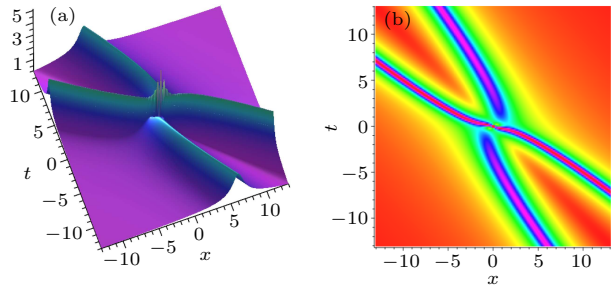


Fig. 3. Dynamic evolution diagram of the second-order rational traveling solution $|q_{2-\mathrm{rational}}|^2$ of the TOFGI equation on the (x,t)-plane, with $\beta_1=0.64$.

Letting $n=3$ and $n=4$ in Eq. (10) we can obtain a three-positon solution and a four-positon solution, respectively. The plots of the two-positon, three-positon, and four-positon are depicted in Figs. 4, 5, and 6, respectively. The trajectory and attributes of the positon solution will be discussed in the following section.

3. Dynamics of the positons

From the three-dimensional evolution diagram of the positon solution, we can see that the trajectory of the positon solution is a curve, which is different from the trajectory of soliton solution which is a straight line. Each soliton can be identified in the particle sense because the N-soliton solution can be split into the sum of n single soliton solutions. The N-positon solution is derived from the degradation of the N-solitons solution and is a nonsingular real solution. It is necessary to verify whether the N-positon solutions also have properties similar to the N-soliton solutions. We split the modulus square of the N-positon solution to analyze its dynamic properties.

Let us start with the two-positon solution. Because splitting the two-positon solution into two single solitons will produce a constant phase shift when $|t|\to\infty$, it is naturally assumed that the splitting of the two-positon as the following when $|t|\to\infty$:

$$|q_{2-p}|^2\approx|q_{1-s}(H+c_1)|^2+|q_{1-s}(H-c_1)|^2.$$

The item $|q_{1-s}(H\pm c_1)|^2$ on the right-hand side can be obtained by Eq. (8)

$$|q_{1-s}(H\pm c_1)|^2=\frac{64\alpha_1^2\beta_1^2\,\mathrm{e}^{8\alpha_1\beta_1(H\pm c_1)}}{(\beta_1^2+\alpha_1^2)(\mathrm{e}^{16\alpha_1\beta_1(H\pm c_1)}+1)-2(\beta_1^2-\alpha_1^2)\,\mathrm{e}^{8\alpha_1\beta_1(H\pm c_1)}}. \tag{13}$$

From Eq. (11), the left-hand side of the equation can be obtained. Letting $H\to 0$, after a series of approximate calculations, the phase shift c_1 yields the following formula:

$$\begin{aligned}&\omega_6 t^4+(\alpha_1^2+\beta_1^2)^2\cosh(16\alpha_1\beta_1 c_1)\\&-16\alpha_1^8+6\beta_1^4-4\alpha_1^2\beta_1^2+6\alpha_1^4\approx 0.\end{aligned} \tag{14}$$

Solving the above formula and getting

$$c_1\approx-\frac{\ln(2^{23}3^4\alpha_1^4\beta_1^4(\alpha_1^2+\beta_1^2)^4(9\beta_1^4-14\alpha_1^2\beta_1^2+9\alpha_1^4)^2t^4)}{16\alpha_1\beta_1},$$

c_1 can be written in a simpler form $c_1\approx-\frac{\ln(2^{23}3^4t^4)}{16\alpha_1\beta_1}$ when $|t|\to\infty$. In summary, the following proposition can be obtained.

Proposition 2 As $|t|\to\infty$, the modulus square of the two-positon solution of the TOFGI equation is split as the following form:

$$|q_{2-p}|^2\approx|q_{1-s}(H+c_1)|^2+|q_{1-s}(H-c_1)|^2, \tag{15}$$

the phase shift generated here is $c_1=-\frac{\ln(2^{23}3^4t^4)}{16\alpha_1\beta_1}$.

In summary, it can be found that the phase shift generated by the splitting of two-positon solution into two single solitons is not a constant but a function related to t. In order to verify the accuracy of the results, we compare the approximate track of the peak track of the soliton solution mode square with the peak track of the positon mode square, as shown in Fig. 4(c). In Fig. 4(c), it is easy to find that the trajectories of the two overlap very well when $|t|\to\infty$. Therefore, the method of splitting the positon solution is very accurate. The three-positon solution can also be split by using the same method.

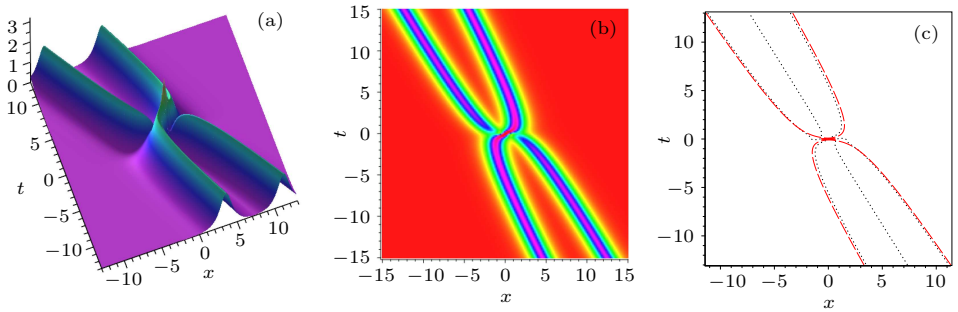


Fig. 4. Dynamic evolution diagram of two-positon solution $|q_{2-p}|^2$ of the TOFGI equation on the (x,t)-plane, with $\alpha_1=0.8$ and $\beta_1=0.4$. (a) and (b) The three-dimensional diagram and density diagram of the two-positon solution, respectively. (c) The black dotted line is the extreme trajectory of the two-positon solution, and the red broken lines are the approximate trajectory of decomposition.

Assume that when $|t|\to\infty$, the three-positon solution has the following decomposition:

$$|q_{3-p}|^2\approx|q_{1-s}(H+c_2)|^2+|q_{1-s}(H)|^2+|q_{1-s}(H-c_2)|^2,$$

the modulus squares of three-soliton solution and one-soliton solution are brought into the above equation, respectively, and let $H\to 0$. Then, the formula is simplified so that c_2 satisfies the following formula:

$$\begin{aligned}&\omega_7 t^8-4\beta_1^2(\alpha_1^2+\beta_1^2)^2\cosh(16\alpha_1\beta_1 c_2)+2^7\alpha_1^{18}\\&-24\beta_1^6+16\alpha_1^2\beta_1^4-24\alpha_1^4\beta_1^2\approx 0.\end{aligned} \tag{16}$$

Solving Eq. (16) and getting

$$c_2\approx-\frac{\ln\left(2^{44}3^8\alpha_1^{10}\beta_1^{14}(\alpha_1^2+\beta_1^2)^8(9\beta_1^4-14\alpha_1^2\beta_1^2+9\alpha_1^4)^4t^8\right)}{16\alpha_1\beta_1},$$

c_2 can also be written in a simpler form $c_2\approx-\frac{\ln(2^{44}3^8t^8)}{16\alpha_1\beta_1}$. Therefore, we can get the following proposition.

Proposition 3 As $|t|\to\infty$, the modulus square of the three-positon solution of the TOFGI equation is split as the following form:

$$\begin{aligned}|q_{3-p}|^2\approx{}&|q_{1-s}(H+c_2)|^2+|q_{1-s}(H)|^2\\&+|q_{1-s}(H-c_2)|^2,\end{aligned} \tag{17}$$

the phase shift generated here is $c_2=-\frac{\ln(2^{44}3^8t^8)}{16\alpha_1\beta_1}$.

The dynamic plot of the three-positon solution is given in Fig. 5(c). It can be seen from the figure that the approximate orbit of the mode square peak trajectory of the soliton solution overlaps well with the positon mode square peak trajectory when $|t|\to\infty$. The higher-order positon solution can still be split by the same method. For simplicity, the decomposition of the multi-positon solution is omitted.

Remark 2 The phase shift generated by the decomposition of the two-positon solution of the GI equation is equivalent to $\ln t^2$, and the phase shift generated by the decomposition of the three-positon solution is equivalent to $\ln t^4$.[36] The phase shift generated by the decomposition of the two-positon solution of the TOFGI equation is equivalent to $\ln t^4$, and the phase shift generated by the decomposition of the three-positon solution is equivalent to $\ln t^8$. It shows that the phase shift generated by the decomposition of the N-positon solution of the higher-order NLS equation into the single soliton solution is more affected by t, but we can also identify each positon solution from the particle sense.

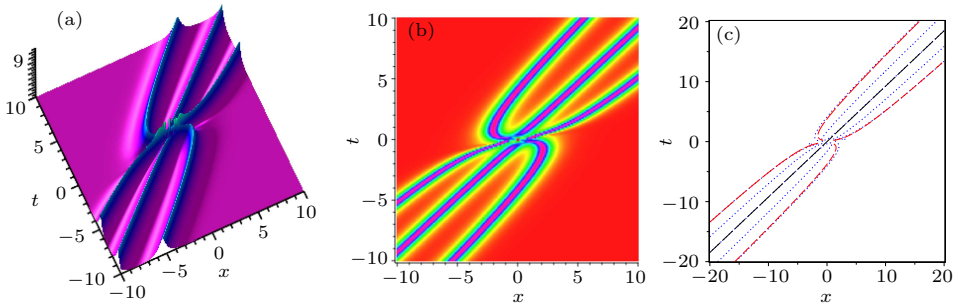


Fig. 5. Dynamic evolution diagram of the three-positon solution $|q_{3-p}|^2$ of the TOFGI equation on the (x,t)-plane, with $\alpha_1 = 4/7$ and $\beta_1 = 4/5$. (a) and (b) The three-dimensional diagram and density diagram of the three-positon solution, respectively. (c) The blue dots curve is the extreme trajectory of the three-positon solution, the black dotted line ($H = 0$) in the middle is the trajectory without phase shift, and the red broken curves are the approximate trajectory with phase shift of decomposition.

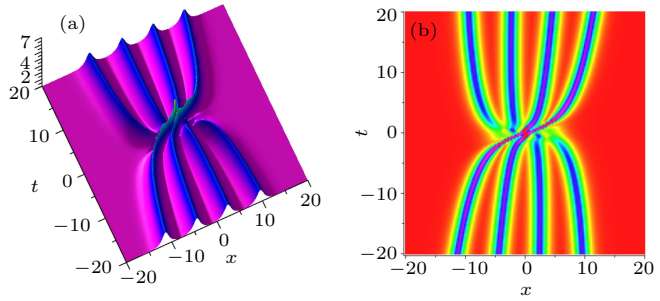


Fig. 6. The dynamics of the four-positon solution modulus square of the TOFGI equation on the (x,t) plane. (a) and (b) The three-dimensional plot and two-dimensional plot with $\alpha_1 = 0.75$, $\beta_1 = 0.44$, respectively.

4. The breather solutions of the TOFGI equation

By substituting the non-zero seed solution $q = c\,\mathrm{e}^{\mathrm{i}(ax+bt)}$ into Eq. (2), where a and b are constants, $b = -\frac{3}{4}ac^4 + \frac{3}{2}a^2c^2 + \frac{1}{2}a^3$ can be obtained. Then, $q = c\,\mathrm{e}^{\mathrm{i}(ax+(-\frac{3}{4}ac^4+\frac{3}{2}a^2c^2+\frac{1}{2}a^3)t)}$ is substituted into Eq. (4) of the spectral problem, and the results are obtained by using the method of separating variables and the superposition principle, the eigenfunction ϕ_j associated with λ_j is given by

$$\begin{pmatrix} f_j(x,t,\lambda_j) \\ g_j(x,t,\lambda_j) \end{pmatrix} = \begin{pmatrix} \varpi^1_{1j}(x,t,\lambda_j) + \varpi^2_{1j}(x,t,\lambda_j) + \varpi^1_{2j}{}^*(x,t,-\lambda_j^*) + \varpi^2_{2j}{}^*(x,t,-\lambda_j^*) \\ \varpi^1_{2j}(x,t,\lambda_j) + \varpi^2_{2j}(x,t,\lambda_j) + \varpi^1_{1j}{}^*(x,t,-\lambda_j^*) + \varpi^2_{1j}{}^*(x,t,-\lambda_j^*) \end{pmatrix}, \tag{18}$$

where

$$\begin{aligned}
\begin{pmatrix} \varpi^1_{1j}(x,t,\lambda_j) \\ \varpi^1_{2j}(x,t,\lambda_j) \end{pmatrix} &= \begin{pmatrix} \exp\left(\dfrac{\sqrt{s}[(8\lambda_j^4 - 4a\lambda^2 + 2ac^2 + 2a^2)t + 4x]}{8} + \dfrac{\mathrm{i}\left[\left(-\dfrac{3}{2}ac^4 + 3a^2c^2 + a^3\right)t + 2ax\right]}{4}\right) \\ \dfrac{\sqrt{s} - \mathrm{i}c^2 + s\mathrm{i}\lambda_j^2 + \mathrm{i}a}{2c\lambda_j} \exp\left(\dfrac{\sqrt{s}[(8\lambda_j^4 - 4a\lambda_j^2 + 2ac^2 + 2a^2)t + 4x]}{8} - \dfrac{\mathrm{i}\left[\left(-\dfrac{3}{2}ac^4 + 3a^2c^2 + a^3\right)t + 2ax\right]}{4}\right) \end{pmatrix}, \\
\begin{pmatrix} \varpi^2_{1j}(x,t,\lambda_j) \\ \varpi^2_{2j}(x,t,\lambda_j) \end{pmatrix} &= \begin{pmatrix} \exp\left(\dfrac{-\sqrt{s}[(8\lambda_j^4 - 4a\lambda^2 + 2ac^2 + 2a^2)t + 4x]}{8} + \dfrac{\mathrm{i}\left[\left(-\dfrac{3}{2}ac^4 + 3a^2c^2 + a^3\right)t + 2ax\right]}{4}\right) \\ \dfrac{-\sqrt{s} - \mathrm{i}c^2 + s\mathrm{i}\lambda_j^2 + \mathrm{i}a}{2c\lambda_j} \exp\left(-\dfrac{\sqrt{s}[(8\lambda_j^4 - 4a\lambda_j^2 + 2ac^2 + 2a^2)t + 4x]}{8} - \dfrac{\mathrm{i}\left[\left(-\dfrac{3}{2}ac^4 + 3a^2c^2 + a^3\right)t + 2ax\right]}{4}\right) \end{pmatrix}, \\
\varpi^1(x,t,\lambda_j) &= \begin{pmatrix} \varpi^1_{1j}(x,t,\lambda_j) \\ \varpi^1_{2j}(x,t,\lambda_j) \end{pmatrix}, \quad \varpi^2(x,t,\lambda_j) = \begin{pmatrix} \varpi^2_{1j}(x,t,\lambda_j) \\ \varpi^2_{2j}(x,t,\lambda_j) \end{pmatrix}, \quad s = -c^4 - 4\lambda_j^4 + 2ac^2 - 4a\lambda_i^2 - a^2.
\end{aligned} \tag{19}$$

Here, $\varpi^1(x,t,\lambda_j)$ and $\varpi^2(x,t,\lambda_j)$ are linearly independent solutions of Eq. (4) of the spectral problem. The breather solution of the TOFGI equation can be obtained by the DT of even order.

For $n = 2$, assuming $\lambda_1 = \alpha_1 + \mathrm{i}\beta_1$, $\lambda_2 = -\lambda_1^*$, and substituting the corresponding eigenfunction (18) into Eq. (5). To simplify the calculation, taking $a = -2\alpha_1^2 + \beta_1^2$ so that $\mathrm{Im}(-c^4 - 4\lambda_1^4 + 2ac^2 - 4a\lambda_1^2 - a^2) = 0$. Thus, the one-breather solution of the TOFGI equation is obtained as follows:

$$\begin{aligned}
q^{[2]}_{\text{breather}} &= \exp\left(-4\mathrm{i}S\left(\frac{x}{2} + \left(S^2 - \frac{3}{2}c^2S - \frac{3}{8}c^4\right)t\right)\right) \\
&\quad \times \left(-c + \frac{u_1}{u_2}\right),
\end{aligned} \tag{20}$$

where

$$u_1 = 2(4\alpha_1^2 + c^2)\left(-2\mathrm{i}\beta_1 K\sin(f_2) + \alpha_1(-8\beta_1^2 + 2c^2)\cos(f_2)\right),$$

$$
\begin{aligned}
u_2 &= -2\mathrm{i}c\beta_1 K\sin(f_2)+(8\alpha_1^3 c+2\alpha_1 c^3)\cos(f_2)\\
&\quad -4\mathrm{i}\alpha_1\beta_1 K\sinh(f_1)-(16\alpha_1^3\beta_1+4\alpha_1\beta_1 c^2)\cosh(f_1),\\
f_1 &= \frac{1}{4}K((-24\alpha_1^4+(80\beta_1^2+4c^2)\alpha_1^2+c^4\\
&\quad -4\beta_1^2 c^2-24\beta_1^4)t-4x),\\
f_2 &= 12K\alpha_1\beta_1(\alpha_1^2-\beta_1^2)t,\\
K &= \sqrt{(4\beta_1^2-c^2)(4\alpha_1^2+c^2)},\quad S=\alpha_1^2-\beta_1^2.
\end{aligned}
$$

When $t\to\infty$ and $x\to\infty$, $|q^{[2]}_{\text{breather}}|^2\to c^2$. In addition, the trajectory of the one-breather solution is determined by $f_1=0$ when $s>0$, $x=(\frac{1}{4}c^4-6\alpha_1^4+20\alpha_1^2\beta_1^2+\alpha_1^2c^2-6\beta_1^4-\beta_1^2c^2)t$. When $s<0$, the trajectory of the one-breather solution is determined by $f_2=0$ as $t=0$.

Thus, the one-breather solution of time periodic and the one-breather solution of space periodic of the TOFGI equation can be obtained. When taking the parameters that meet the above conditions, Figs. 7(a) and 7(b) show the dynamic behavior of their time periodic and space periodic solutions Eq. (20) respectively. In Fig. 7(c), the dynamic evolution structure of the one-breather solution in general is given, and its trajectory is a periodic motion of a straight line on the (x,t) plane.

For $n=4$, assume $\lambda_1=\alpha_1+\mathrm{i}\beta_1$, $\lambda_2=-\lambda_1^*$, $\lambda_3=\alpha_3+\mathrm{i}\beta_3$, $\lambda_4=-\lambda_3^*$, using the same method as above, we can obtain the two-breather solution $q^{[4]}$ of the TOFGI equation after four-fold DT. Here, it is omitted the complex expression of the two-breather solution, but its dynamic evolution is given in Fig. 7(d).

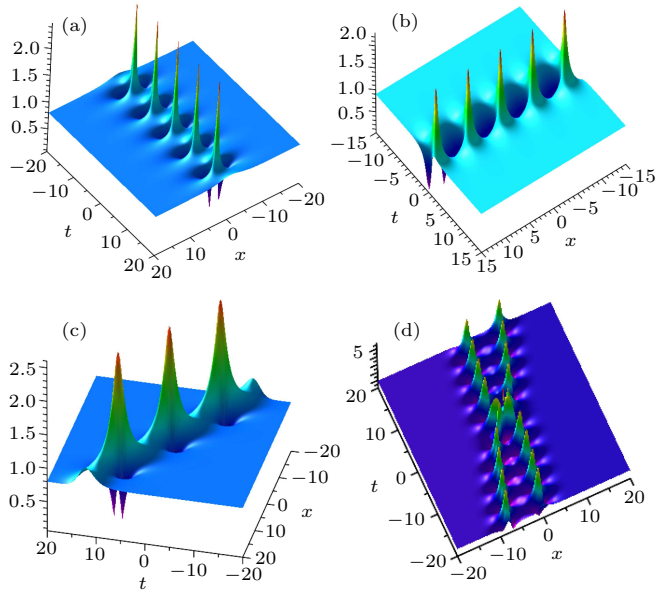


Fig. 7. (a) The first-order breather solution of time period $|q^{[2]}_{\text{breather}}|^2$ of the TOFGI equation with $\alpha_1=4/5$, $\beta_1=2\sqrt{57-3\sqrt{247}}/15$, $c=4/5$ and the trajectory is a line $x=0$. (b) The first-order breather solution of space period with $\alpha_1=0.7$, $\beta_1=0.35$, $c=0.9$, and the trajectory is a line $t=0$. (c) The general first-order breather solution with $\alpha_1=0.66$, $\beta_1=0.45$, $c=0.8$. (d) The second-order breather solution $|q^{[4]}|^2$ with $\alpha_1=0.45$, $\beta_1=0.7$, $\alpha_3=0.44$, $\beta_3=0.71$, $c=1$.

Remark 3 From the analytical expression and dynamic evolution of the one-breather solution of the TOFGI equation, we can clearly find that its motion trajectory and propagation speed are completely different from the corresponding solution of the GI equation under the same condition, which is the same as that in remark 1 above. It can be concluded that the higher-order nonlinear terms in the TOFGI equation will affect the propagation speed and motion trajectory of the solution.

5. Conclusions

In this paper, some exact solutions and properties of the TOFGI equation with higher-order nonlinear terms are studied. In Section 2, the determinant expression of the new solution is obtained in Lemma 1 by using DT. Then, the soliton solution and rational solution are obtained by taking zero seed solution and different spectral parameters. The positon solution of the N-solution of the TOFGI equation is obtained by using the degenerate DT in Proposition 1. The three-dimensional and density diagrams of these solutions are shown in Figs. 1–6, respectively. In Section 3, the dynamical properties of the N-positon solution of the TOFGI equation are studied. The decomposition of the two-positon solution and three-positon solution are obtained in Propositions 2 and 3, and the dynamic evolution diagrams are shown in Figs. 4 and 5. In Section 4, the breather solution of the TOFGI equation is studied. Figure 7 shows the three-dimensional diagram of the breather solution of the TOFGI equation.

Finally, by comparing the soliton and positon solutions of the GI equation and the TOFGI equation, it is found that the propagation velocity of the soliton and positon solutions of these two equations are different, with the opposite propagation direction and the same height of wave peak. Therefore, it can be concluded that the higher-order nonlinear term of the TOFGI equation only affects the propagation velocity and trajectory of the wave, but does not affect the peak value of the wave. The results of this paper have certain reference value and provide possible theoretical support for the study of high-order nonlinear effects and applications of high-order dispersion in the future.

Acknowledgements

Project supported by the National Natural Science Foundation of China (Grant No. 12201329), the Zhejiang Provincial Natural Science Foundation of China (Grant No. LY24A010002), and the Natural Science Foundation of Ningbo (Grant No. 2023J126).

References

[1] Russell J S 1844 *Report on Waves. Report of the 14th Meeting of the British Association for the Advancement of Science* (London)
[2] Korteweg D J and de Vries G 1895 *Philos. Mag.* **39** 422
[3] Gardner C S and Morikawa G K 1960 *Similarity in the asymptotic behavior of collision-free hydromagnetic waves and water waves* (New York University)

[4] Kruskal M D 1965 *Proceedings of the IBM Scientific Computing Symposium on Large-Scale Problems in Physics* (White Plains, New York)
[5] Hasegawa A and Tappert F 1973 *Appl. Phys. Lett.* **23** 142
[6] Hirota R 1973 *J. Math. Phys.* **14** 805
[7] Kundu A 1984 *J. Math. Phys.* **25** 3433
[8] Wang X, Yang B, Chen Y and Yang Y Q 2014 *Phys. Scr.* **89** 095210
[9] Kruglov V I, Peacock A C and Harvey J D 2003 *Phys. Rev. Lett.* **90** 113902
[10] Wang L H, Porsezian K and He J S 2013 *Phys. Rev. E* **87** 053202
[11] Xu S W, He J S and Wang L H 2011 *J. Phys. A-Math. Theor.* **44** 305203
[12] Zhang Y S, Guo L J, Xu S W, Wu Z W and He J S 2014 *Commun. Nonlinear Sci. Numer. Simul.* **19** 1706
[13] Zhang H Q, Liu R and Chen F 2023 *Nonlinear Dyn.* **111** 645
[14] Xiang Y J, Dai X Y, Wen S C, Guo J and Fan D Y 2011 *Phys. Rev. A* **84** 033815
[15] Kaup D J and Newell A C 1978 *J. Math. Phys.* **19** 798
[16] Chen H H, Lee Y C and Liu C S 1979 *Phys. Scr.* **20** 490
[17] Gerdjikov V S and Ivanov M I 1983 *Bulg. J. Phys.* **10** 130
[18] Mjølhus E 1976 *J. Plasma Phys.* **16** 321
[19] Mjølhus E 1989 *Phys. Scr.* **40** 227
[20] Agrawal G P 2000 *Nonlinear fiber optics. Nonlinear Science at the Dawn of the 21st Century* **542** 195
[21] Zhu J Y and Chen Y 2024 *Acta Math. Appl. Sin-E.* **40** 358
[22] Li Y S, Gu X S and Zou M R 1987 *Acta Math. Sin. (New Series)* **3** 143
[23] Matveev V B and Salle M A 1991 *Darboux Transformations and Solitons* (Berlin: Springer)
[24] Gu C H, Hu H S and Zhou Z X 2006 *Darboux Trasformations in Integrable Systems* (Dortrecht: Springer)
[25] He J S, Zhang L, Cheng Y and Li Y S 2006 *Sci. China Ser. A Math.* **49** 1867
[26] Liu J Z, Yan X X, Jin M and Xin X P 2023 *Chin. Phys. B* **32** 120401
[27] Wei J, Geng X G and Wang X 2024 *Chin. Phys. B* **33** 070202
[28] Matveev V B 1992 *Phys. Lett. A* **166** 205
[29] Maisch H and Stahlhofen A A 1995 *Phys. Scr.* **52** 228
[30] Hu H C and Liu Y 2008 *Phys. Lett. A* **372** 5795
[31] Song W J, Xu S W, Li M H and He J S 2019 *Nonlinear Dyn.* **97** 2135
[32] Yuan F and Ghanbari B 2023 *Chin. Phys. B* **32** 075208
[33] Wadati M 1973 *J. Phys. Soc. Jpn.* **34** 1289
[34] Xu S W and He J S 2012 *J. Math. Phys.* **53** 063507
[35] Lin H A, He J S, Wang L H and Mihalache D 2020 *Nonlinear Dyn.* **100** 2839
[36] Yang X, Zhang Z and Li B 2020 *Chin. Phys. B* **29** 100501